



HAL
open science

First-in-Man Noninvasive Initial Diagnostic Approach of Primary CNS Lymphoma Versus Glioblastoma Using PET With 18F-Fludarabine and l-[methyl-11C]Methionine

Andrey Postnov, Jérôme Toutain, Igor Pronin, Valable Samuel, Fabienne Gourand, Diana Kalaeva, Nina Vikhrova, Elena Pyzhik, Stéphane Guillouet, Grigoriy Kobayakov, et al.

► To cite this version:

Andrey Postnov, Jérôme Toutain, Igor Pronin, Valable Samuel, Fabienne Gourand, et al.. First-in-Man Noninvasive Initial Diagnostic Approach of Primary CNS Lymphoma Versus Glioblastoma Using PET With 18F-Fludarabine and l-[methyl-11C]Methionine. *Clinical Nuclear Medicine*, 2022, 47 (8), pp.699-706. 10.1097/RLU.0000000000004238 . hal-03672116

HAL Id: hal-03672116

<https://normandie-univ.hal.science/hal-03672116>

Submitted on 19 Sep 2022

HAL is a multi-disciplinary open access archive for the deposit and dissemination of scientific research documents, whether they are published or not. The documents may come from teaching and research institutions in France or abroad, or from public or private research centers.

L'archive ouverte pluridisciplinaire **HAL**, est destinée au dépôt et à la diffusion de documents scientifiques de niveau recherche, publiés ou non, émanant des établissements d'enseignement et de recherche français ou étrangers, des laboratoires publics ou privés.

**First-in-man non-invasive initial diagnostic approach of primary CNS lymphoma versus glioblastoma
using PET with F-18-fludarabine and L-[methyl-C-11]methionine**

Andrey Postnov PhD^{1,2,3}, Jérôme Toutain MsC⁴, Igor Pronin MD/PhD¹, Samuel Valable PhD⁴, Fabienne Gourand PhD⁵, Diana Kalaeva MD^{1,2}, Nina Vikhrova MD¹, Elena Pyzhik MsC¹, Stéphane Guillouet PhD⁵, Grigoriy Kobayakov PhD¹, Ekaterina Khokholova MD¹, David Pitskhelauri MD¹, Dmitry Usachev MD¹, Sergey Maryashev MD¹, Marina Rizhova MD¹, Alexander Potapov MD PhD¹, Jean-Michel Derlon MD PhD^{1,4}

1. N.N.Burdenko National Medical Research Center of Neurosurgery, Moscow, Russia
2. National Research Nuclear University MEPhI, Moscow, Russia
3. The P.N. Lebedev Physical Institute, Moscow, Russia
4. Normandie Univ, UNICAEN, CNRS, ISTCT, GIP CYCERON, France
5. Normandie Univ, UNICAEN, CEA, CNRS, ISTCT/LDM-TEP group, GIP CYCERON, France

ABSTRACT

This study sought to assess F-18-fludarabine (F-18 FLUDA) PET/CT's ability in differentiating primary central nervous system lymphomas (PCNSL) from glioblastomas (GBM).

Methods: Patients harboring either PCNSL (n=8) before any treatment, PCNSL treated using corticosteroids (PCNSLh; n=10), or GBM (n=13) were investigated with conventional MRI and PET/CT, using C-11 MET and F-18 FLUDA. The main parameters measured with each tracer were SUV_T and T/N ratios for the first 30 min of C-11 MET acquisition, as well as at three different times following F-18 FLUDA injection. The early F-18 FLUDA uptake within the 1st minute of injection was equally considered, while this parameter was combined with the later uptakes to obtain R FLUDA 2 and R FLUDA 3 ratios.

Results: No significant differences in C-11 MET uptakes were observed among PCNSL, PCNSLh, and GBM. With F-18 FLUDA, a clear difference in dynamic GBM uptake was observed, which decreased over time after an early maximum, as compared with that of PCNSL, which steadily increased over time, PCNSLh exhibiting intermediate values. The most discriminative parameters consisting of R FLUDA 2 and R FLUDA 3 integrated the early tracer uptake (first 60 seconds), thereby provided 100% specificity and sensitivity.

Conclusion: F-18 FLUDA was shown to likely be a promising radiopharmaceutical for differentiating PCNSL from other malignancies, though a pretreatment with corticosteroids might compromise this differential diagnostic ability. The diagnostic role of F-18 FLUDA should be further investigating, along with its potential of defining therapeutic strategies in patients with PCNSL, whilst assessing the treatments' effectiveness.

Key words: PET, primary brain lymphoma, glioblastoma, F-18 fludarabine, C-11 methionine

INTRODUCTION

Primary central nervous system lymphomas (PCNSL) are rare intracranial tumors representing approximately 3% of all CNS tumors [1]. Their diagnosis is often challenging, given that on CT or MRI examinations, these tumors share similar features with other malignant tumors, including glioblastomas or metastases. Early identification, before initiating any treatment including corticosteroids, is paramount, given that these tumors do not require surgical removal and respond to specific oncological protocols that differ from those employed for other brain malignancies.

Thus far, when a PCNSL is first suspected, the initial diagnosis must be confirmed by histologic findings. During patient follow-up, other difficulties may arise, such as assessing the response to different treatment protocols, as well as differentiating residual or recurring tumor processes from non-tumor complications like radiation necrosis. Conventional neuro-imaging methods like F-18 fluorodeoxyglucose (F-18 FDG) PET may turn out to be non-effective enough for resolving these issues, due to their lacking specificity.

Fludarabine is an adenine nucleoside analog that is resistant to adenosine deaminase, while linking specifically with B-lymphocytes; this molecule is employed as antitumor agent in managing diverse lymphoid proliferative diseases like follicular lymphomas [2], and in chronic lymphocytic leukemia, as well. The introduction of a fluorine-18 atom has generated a positron-emitting radiotracer, F-18 fludarabine (F-18 FLUDA) [3], which already underwent a first preclinical evaluation [4]. This latter study sought to compare the uptake of F-18 FLUDA with that of F-18 FDG in immune-deficient mice subcutaneously engrafted with subcutaneous follicular lymphoma human xenograft. The analysis demonstrated that the uptake of F-18 FLUDA was selectively much higher in the tumor than in other target organs, whereas the uptake of F-18 FDG was high in both categories of tissues. In a preclinical model of inflammation in mice [5], the uptake of F-18 FLUDA was, however, demonstrated to be significantly weaker than that of F-18 FDG. The first clinical assessment of the tracer was performed involving 10 patients, half of them harboring a peripheral diffuse large B-cell lymphoma (DLBCL) and the other half a chronic lymphocytic leukemia [6]. In DLBCL, the SUV_{max} values of all tumor sites were significantly higher than those of other tissues, and this over the full acquisition time. Based on these preliminary results, F-18 FLUDA was suggested to be capable of differentiating PCNSL from other brain malignancies. A preclinical study [7] compared the uptake of both F-18 FLUDA and F-18 FDG in nude rats that were cerebrally implanted with either human lymphoma-cells or glioma cells. With F-18 FLUDA, the tumor to background ratio (TBR) was markedly higher

in PCNSL than glioblastoma multiforme (GBM), without any overlap between the two populations, whereas this difference was less pronounced when using F-18 FDG.

The current study sought to further assess the accuracy of F-18 FLUDA in differentiating PCNSL from GBM in humans. In this work, the uptake of F-18 FLUDA was compared with that of L-[*methyl*-¹¹C]methionine (C-11 MET), this latter being commonly used as reference tracer for investigating benign and aggressive brain tumors including lymphomas [8].

MATERIALS AND METHODS

Patients

Overall, 31 patients (18 males and 13 females; mean age: 59.83 years) were included in the study, which was carried out from April 2019 to November 2020. The investigation protocol was approved by the Local Ethical Committee (recorded in 10/2018), and all patients provided their informed consent to participate to the study. Each patient had been submitted to either stereotactic biopsy, when the tumor was thought to most likely be a PCNSL or presented with a deep location, or to open surgery consisting of tumor removal when the results favored a GBM, its location was deemed suitable for such a removal. Using histomolecular criteria and according to the World Health Organization (WHO) classification of brain tumors [9], overall 18 PCNSL and 13 GBM were considered for diagnosis. Among the PCNSL patients, eight did not receive any previous treatment (named PCNSL), whereas 10 (named PCNSLh) had previously been given dexamethasone, using variable dosages and treatment durations (see appendix), which was then discontinued a few days before the investigations. Among the GBM patients, one unique patient received dexamethasone prior to the investigations. As a result, we defined the following three patient groups, which were all analyzed prospectively: **Group 1=PCNSL; Group 2= PCNSLh; Group 3=GBM.**

Image acquisition

Each patient underwent a full imaging investigation, including MRI, as well as PET/CT with two different tracers, C-11 MET and F-18 FLUDA. The full investigations, consisting of MRI and PET/CT imaging, shortly followed by tissue sampling and morphological diagnosis, were performed within maximally five days.

MRI: MRI was performed on a 1.5 Tesla Optima 450 (GE Healthcare, Boston, USA) comprising the following sequences: 3DT1w before and after contrast agent injection (Gadobutrol 0.1mmol/Kg, BAYER, Leverkusen, Germany), T2w, and FLAIR.

After MRI, the patients underwent two PET investigations (Biograph Truepoint, Siemens Medical Solutions, Knoxville, USA) with F-18 FLUDA and C-11 MET, synthesized as previously described [10, 4]

PET: C-11 MET-PET was performed on a patient having fasted for at least 4 hours, after an intravenous injection of $3.22 \pm 0.5 \text{ MBq/Kg}$ ($0.087 \pm 0.013 \text{ mCi/Kg}$) C-11 MET with an acquisition time of 30 min. Data acquisition started at the time of injection. The dynamic series consisted of 26 frames with the duration of $6 * 10 \text{ sec}$, $6 * 20 \text{ sec}$, $6 * 30 \text{ sec}$, $4 * 60 \text{ sec}$ and $8 * 150 \text{ sec}$.

For F-18 FLUDA, three successive PET scans were acquired, up to 120 min after an intravenous injection of $4.05 \pm 0.26 \text{ MBq/Kg}$ ($0.109 \pm 0.007 \text{ mCi/Kg}$) F-18 FLUDA. The first scan was performed at 10 minutes (22 frames) (FLUDA1). Two more data acquisitions were carried out at 40-60 minutes (FLUDA2) and 100-120 minutes (FLUDA3), respectively, each reconstructed with four frames of 5 minutes. The OSEM 3D algorithm (five iterations and eight subsets) was applied for the reconstruction. Low-dose CT scan was conducted for attenuation correction.

Image analysis

SUV (standardized uptake values) images were computed as follow: $\text{SUV (g/mL)} = \text{local tissue activity (kBq/mL)} / [\text{injected dose (kBq)/weight (g)}]$.

All PET images were co-registered to the 3D-T1 images with PMOD software using rigid matching registration. The volume of interest (VOI_T) was a volume of 1 cm^3 connected voxels with the highest uptake, which were automatically delineated on averaged images from 5 to 10 minutes for F-18 FLUDA and from 10 to 30 minutes for C-11 MET. The VOI (VOI_N) of the normal appearing tissue was selected as a sphere with a diameter of 16mm in the frontal lobe of the contralateral hemisphere, including a mix of gray and white matter.

For F-18 FLUDA-PET images, the ratio $\text{SUV}_T/\text{SUV}_N$ was calculated (T/N FLUDA), as well as the SUV change between the early (FLUDA1) and latest (FLUDA3) acquisition periods: $\text{FLUDA change \%} = (\text{FLUDA 3} - \text{FLUDA 1}) / (\text{FLUDA 1} \times 100)$. To analyze the first tracer pass through the tumor, the uptake ratios were calculated for the first 60 seconds p.i. (T/N60). Next, the ratios of T/N60 to T/N, hereinafter referred to as R (R FLUDA 2 and R FLUDA 3) were additionally calculated.

For C-11 MET-PET images, SUV values were measured in VOI_T and VOI_N , respectively, with T/N ratio calculated. The ability of C-11 MET to differentiate between GBM (10 out of 13 patients with full dynamic data were included, whereas three patients displayed shorter C-11 MET acquisitions due to technical reasons) and PCNSL (all eight patients included) as assessed using the approach reported by Kawase et. al [11]. As a result, we

checked the discriminating power of $\Delta\text{SUV}_{\text{max}}$ while comparing early and later uptakes, with $\Delta\text{SUV}_{\text{max}} = \text{averaged SUV}_{(20-30 \text{ min})} / \text{averaged SUV}_{(0-20 \text{ min})}$.

Statistical analyses

All statistical analyses were performed using JMP13 (SAS, USA). For the three time points analyzed for F-18 FLUDA, ANOVA followed by HSD Tukey post-hoc testing was applied. The performance of each parameter to discriminate PCNSL from GBM was measured by means of receiver operating characteristic (ROC) analyses.

RESULTS

The results and statistics for the three different groups are displayed in Tables 1 and 2.

As expected, all patients from the three groups (PCNSL, PCNSLh and GBM) displayed a pronounced contrast agent enhancement (Panel A of Figures 1 and 2). All the tumors in each group exhibited a high C-11 MET uptake (Panel B of Figure 1 and 2, Table 1) concerning both SUV values and T/N ratios, whereas these values did not significantly differ among groups (Table 2).

On visual inspection of PCNSL cases, F-18 FLUDA uptake was pronounced in the MRI enhancement region at Time 1 (Figure 1). An uptake was similarly detected in the bones and healthy brain tissues. Thereafter, the uptake gradually declined in the healthy regions, whereas it increased in the tumor region over time (Figure 1D/E). An almost similar uptake was observed in the PCNSLh group, whereas the subsequent uptake was variable among cases. In contrast, concerning the GBM group (Figure 2), the initial uptake within the tumor was lower than that observed in patients with PCNSL and PCNSLh, followed by a gradual decline with time. These dynamic changes are clearly observable on Figure 3.

At Time 0-10 min (FLUDA 1), SUV values were significantly higher in PCNSL and PCNSLh versus GBM (Table 1 and 2, and Figure 3). At Time 40-60 min (FLUDA 2), the difference was more pronounced, becoming statistically significant between GBM and PCNSL. At Time 100-120 min (FLUDA 3), the differences in SUV values were again higher among the three groups (Tables 1 and 2; Figure 3). Almost similar results and statistics were obtained for T/N ratios, while FLUDA changes were less significant among groups (Tables 1 and 2).

It should be noted that no significant differences were observed in normal brain tissues among the three groups.

The integration of the perfusion factor T/N60 accurately discriminated PCNSL from GBM, concerning not only the T/N60 ratio itself, but more particularly the R FLUDA 2 and R FLUDA 3 (Tables 1 and 2).

Considering the C-11 MET data, we observed a pronounced difference among groups ($\Delta\text{SUV}_{\text{max}}=1.06\pm 0.07\text{g/mL}$ for GBM and $1.18\pm 0.05\text{g/mL}$ for PCNSL, $p=0.001$, Table 2), resulting in identification in tumor groups with 80% specificity and 100% sensitivity of an area under curve (AUC)=0.9, at a cutoff 1.10 (Table 3). We were thus unable to reach absolute discrimination based on $\Delta\text{SUV}_{\text{max}}$, which might be explained by reduced scanning time (30 minutes in our experiment vs. 40 minutes in the original research [11]). Likewise, averaged T/N and $\Delta\text{SUV}_{\text{max}}$ curves (Fig. 6) demonstrated a clear difference in C-11 MET uptake between GBM and PCNSL, at both early and late time points.

As this study's primary objective was to compare the ability of F-18 FLUDA in discriminating PCNSL from GBM, we subsequently performed ROC studies between these two groups (Table 3). For SUV FLUDA 3, AUC was 0.923 and the cutoff 2.43g/mL, with 75% sensitivity and 75% specificity. For T/N FLUDA3, AUC was 0.961 and the cutoff 4.51g/mL, with 87.5% sensitivity and 80% specificity. FLUDA change resulted in AUC of 0.942 and the cutoff -8.943% , with 100% sensitivity and 76.9% specificity. Particularly discriminating were the parameters that included the perfusion factor T/N60, namely R FLUDA 2 and R FLUDA 3, given that we obtained with both an AUC at 1, thus resulting in both 100% sensitivity and specificity for differentiating PCNSL from GBM. This can be clearly seen on Figures 4 and 5, with individual results of the three different tumor groups. It was only with the parameters that included the perfusion factor T/N60 that here was no overlap between the values pertaining to GBM and PCNSL cases. This was not observed with any parameter that omitted including perfusion information (Figure 4) or with the C-11 MET data, even concerning $\Delta\text{SUV}_{\text{max}}$, as can be seen on Fig. 6.

DISCUSSION

Our study aimed to assess the diagnostic accuracy of F-18 FLUDA in PCNSL in such a way that for future investigations, this tracer if given in association with other imaging methods would render diagnostic morphologic confirmation by tissue removal unnecessary. We compared the F-18 FLUDA uptake in PCNSL with that observed GBM, which is the most commonly encountered and most challenging differential diagnosis. While conventional and advanced MRI biomarkers were shown to display a good behavior in differentiating PCNSL from GBM [12, 13], the MRI biomarkers' main limitation is the lack of specificity to tumor cells. In our study, we did not use advanced MR imaging, since the aim was to evaluate the capacity of PET in differentiating PCNSL from GBM.

A number of publications have previously reported on using F-18 FDG for tracing PCNSL, as well as other brain malignancies. Kosaka *et al.* [14] found that SUVmax was the most discriminating parameter. However, other publications [15, 11, 16] reported rather variable SUVmax values in their PCNSL patients. Yamashita *et al.* [17] similarly found that SUVmax was significantly higher in PCNSL compared with GBM, yet once again, with a mild overlap of values measured in both groups. In their meta-analysis involving eight retrospective studies, Zou *et al.* [18] revealed that median SUVmax was highly variable, with a good diagnostic performance. In a large series involving 92 patients, Zhou *et al.* [19] concluded that SUVmax exhibited the highest sensitivity (92.31%) and T/N ratio the highest specificity (92.31%) for the differential diagnosis.

Fewer publications reported on using C-11 MET [20] in the assessment of PCNSL. Only one study [21] compared this tracer to ¹⁸F-FDG for establishing the differential diagnosis between 15 patients with GBM and seven with PCNSL. In this study using F-18 FDG, SUVmax was revealed to significantly correlate with the tumor type. When using C-11 MET, SUVmax did not significantly differ between both groups, though it tended to be lower in patients with GBM compared with PCNS patients. However, $\Delta\text{SUVmax} = \text{SUVmax}_{\text{late phase}} / \text{SUVmax}_{\text{early phase}}$ turned out to be a very discriminative parameter. Another study [22] compared C-11 MET uptake with that of F-18 FDG, yet only involving a population of 13 patients with PCNSL.

Other radiopharmaceuticals in use for the investigation of brain tumors (F-18 thymidine [F-18 FLT], F-18 fluorodopa [F-18 DOPA], F-18 fluoroethyl-L tyrosine [F-18 FET]) have not yet been reported to be appropriate tools for investigating PCNSL [2, 23]. The Ga-68pentixafor, which is a tracer binding to the CXCR4 chemokine receptor, was similarly used for investigating GBM [24] and PCNSL [25], whereas no study to date compared its uptake in both tumor types. We can therefore conclude that by combining advanced MRI sequences with using a PET radiopharmaceutical – either F-18 FDG or C-11 MET –, PCNSL differentiation from other brain malignancies could be rendered possible, with high probability. However, owing to the lack of definitive cutoff values for separating the different tumor varieties, a diagnostic confirmation by biopsy is still mandatory, while there are still doubts, at least in some cases, about the significance of tracer uptake changes during the treatment.

We have therefore designed this preliminary prospective study to compare the uptake of F-18 FLUDA in PCNSL and GBM, respectively. Our protocol was different from that of the first clinical study performed in peripheral lymphomas [6] with respect to acquisition time. Indeed, depending on our considerations, repeated acquisitions over 250 min would turn out to be rather exhausting for patients suffering from brain tumors. Another of our objectives was to compare the uptake of F-18 FLUDA with that of C-11 MET, the latter being considered to accumulate more selectively in tumor tissues than F-18 FDG.

These results are rather encouraging, as they truly confirm that the uptake of F-18 FLUDA is higher in patients with PCNSL than in those suffering from GBM. The most crucial observation was that in patients with PCNSL, this uptake regularly increased from tracer injection up to 120 min, whereas a decreased uptake occurred in patients with GBM. For this reason, we initially thought that the parameter named FLUDA change, reflecting this dynamic uptake, would be the most discriminating parameters in regard to both tumor groups. However, this parameter did not turn out to be superior to the mere SUV_{peak} during the last acquisition time (SUV FLUDA 3). Moreover, even with this parameter, we were unable to achieve 100% accuracy. One explanation for this could be the low number of patients enrolled, with one borderline patient strongly impacting the ROC results. Among the 18 patients with PCNSL, 10 had been treated with dexamethasone before their inclusion. As it has been well known for long, that steroid administration, even at low doses or for short durations, deeply changes the tumor properties, including their histological aspect, we decided include these patients into a third group (PCNSLh). Indeed, for this third group, PET data were clearly intermediate, thereby intermingling with those of the “pure” cases. This major issue is clearly the resultant from the routine clinical practice, which consists of prescribing corticosteroids as soon as an expansive tumor is identified in the brain, before awaiting any confirmation of its nature. Therefore, increasing the number of untreated PCNSL cases might increase the power of our results. Another explanation could be the time at which last uptake of F-18 FLUDA was being measured in our study. In the study performed involving peripheral lymphomas [6], in some patients, the tracer uptake was observed to steadily increase up to 240-250 min of acquisition. In future investigations, we would rather perform three acquisitions, at 0-10 min, 100-120 min, and 240-250 min, which might result in a better discrimination.

Concerning the comparison of our results with those presented in the literature, we should include in the panel of future investigations certain items like advanced MRI imaging, which are now routinely used. These methods further emphasized the relevance of tissue perfusion for differentiating various tumor types. Of note is that this point was further confirmed in our study by introducing the early tracer uptake, within the first 60 seconds of injection, into our calculations, whereas the ratio T/N₆₀, itself, did not appear so discriminating. However, its association with the late uptakes, namely into the R FLUDA 2 and R FLUDA 3 ratios, a clear differentiation between GBM and PCNSL was rendered possible.

Analyzing the dynamic C-11 MET data confirmed that this last tracer exhibited a good potential for differentiating various tumor types. Nevertheless, given that its labelling isotope displays a short half-life, this tracer is most likely to be less suitable than F-18 FLUDA for being routinely employed PET units that are not yet equipped with a cyclotron.

CONCLUSION

Based on this prospective study, we conclude that assessing the dynamic F-18 FLUDA uptake, which was shown to increase over time in patients with PCNSL, whilst decreasing in those with GBM, could become – if confirmed in a larger number of patients - a highly discriminative method for differentiating these categories of brain tumors, without necessitating any invasive histological assessment.

REFERENCES

1. Hoang-Xuan K, Bessell E, Bromberg J, et al. Diagnosis and treatment of primary CNS lymphoma in immunocompetent patients: guidelines from the European Association for Neuro-Oncology. *Lancet Oncol.* 2015; 16: e322–32
2. Anderson V and Perry C. Fludarabine. A review of its use in non-Hodgkin's lymphoma. *Drugs.* 2007; 67:1633-1657
3. Guillouet S, Patin D, Tirel O, et al. Fully automated radiosynthesis of 2-F-18 Fludarabine for PET Imaging of Low-Grade Lymphoma. *Mol Imaging Biol.* 2014; 16:28-35
4. Dhilly M, Guillouet S, Patin D, et al. 2-F-18 Fludarabine, a novel Positron Emission Tomography (PET) tracer for imaging lymphoma: a micro-PET study in murine models. *Mol Imaging Biol.* 2014;16: 118-126
5. Hovhannisyanyan N, Dhilly M, Guillouet S, et al. Comparative analysis between F-18 Fludarabine-PET and F-18 FDG-PET in a murine model of inflammation. *Mol Pharmaceutics.* 2016;13: 2136-2139
6. Chantepie S, Hovhannisyanyan N, Guillouet S, et al. F-18 Fludarabine PET for Lymphoma Imaging: First-in-Humans Study on DLBCL and CLL Patients. *Journal of Nuclear Medicine.* 2018; 59 (9): 1380-1385
7. Hovhannisyanyan N, Fillesoye F, Guillouet S, et al. F-18 Fludarabine-PET as a promising tool for differentiating CNS lymphoma and glioblastoma: Comparative analysis with F-18 FDG in human xenograft models. *Theranostics.* 2018; 8(16): 4563-4573.
8. Derlon JM, Chapon F, Noël MH, et al. Non-invasive grading of oligodendrogliomas: correlations between in vivo metabolic pattern and histopathology. *Eur J Nucl Med.* 2000 ; 27: 778-787
9. D.N. Louis, A. Perrie, P. Wesseling, et al. The 2021 WHO classification of tumours of the Central Nervous System: a summary. *Neuro-Oncology XX(XX)* 2021; 1-21
10. Quincoces G, Lopez-Sanchez L, Sanchez-Martinez M, Rodriguez Fraile M, Penuelas I. Design and performance evaluation of single-use whole-sterile “plug & play” kits for routine automated production of C-11 choline and C-11 methionine with radiopharmaceutical quality. *Appl Radiat Isot.* 2010; 68:2298–2301
11. Kawase Y, Yamamoto Y, Kameyama R, et al. Comparison of C-11 Methionine PET and F-18 FDG PET in patients with Primary Central Nervous System Lymphoma. *Mol Imaging Biol.* 2011; 13: 1284-1289
12. Haldorsen IS, Espeland A, Larsson EM. Central Nervous System Lymphoma: characteristic findings on traditional and advanced imaging. *AJNR.* 2011; 32: 984-992

13. Barajas Jr RF, Letterio S, Politi LS, et al. Consensus recommendations for MRI and PET imaging of primary central nervous system lymphoma: guideline statement from the International Primary CNS Lymphoma Collaborative Group (IPCG). *Neuro-Oncology*. 2021; XX(XX), 1-16
14. Kosaka N, Tsuchida T, Uematsu, et al. F-18 FDG PET of common enhancing malignant brain tumors. *AJR*. 2008; 190: W365-W369
15. Kawai N, Zhen HN, Miyake K, et al. Prognostic value of pretreatment F-18 FDG PET in patients with primary central nervous system lymphoma: SUV-based assessment. *J Neurooncol*. 2010 ;100: 225-232
16. Makino K, Hirai T, Nakamura H, et al. Does adding F-18 FDG PET to MRI improve the differentiation between primary cerebral lymphoma and glioblastoma? Observer performance study. *Annals of Nuclear Medicine*. 2011; 25(6): 432-438
17. Yamashita K, Yoshiura T, Hiwatashi A, et al. Differentiating primary CNS lymphoma from glioblastoma multiforme: assessment using arterial spin labelling, diffusion-weighted imaging, and F-18 fluorodeoxyglucose positron emission tomography. *Neuroradiology*. 2013; 55: 135-143
18. Zou Y, Tong J, Leng H, et al. Diagnostic value of using F-18 FDG PET and PET/CT in immunocompetent patients with primary central nervous system lymphoma: A systematic review and meta-analysis. *Oncotarget*. 2017; 8: 41518-41528
19. Zhou W, Wen J, Hua F, et al. F-18 FDG PET/CT in immunocompetent patients with primary central nervous system lymphoma: Differentiation from glioblastoma and correlation with DWI. *European Journal of Radiology*. 2018; 104: 26-32
20. Comar D, Cartron JC, Mazière M, et al. Labelling and metabolism of L-[methyl-¹¹C]Methionine. *Eur J Nucl Med*. 1976; 1, 11-14
21. Okada Y, Nihashi T, Fujii M, et al. Differentiation of newly diagnosed glioblastoma multiforme and intracranial diffuse large B-cell lymphoma using C-11 Methionine and F-18 FDG PET. *Clin Nucl Med*. 2012; 37: 843-849
22. Ogawa T, Kanno I, Hatazawa J, et al. C-11 Methionine PET for follow-up of radiation therapy of Primary Lymphoma of the Brain. *RadioGraphics*. 1994; 14: 101-110
23. Costantini DL, Reza Vali R, McQuattie S, et al. A pilot study of F-18 FLT PET/CT in pediatric lymphoma. *Int J Mol Imaging*. 2016; 6045894
24. Lapa C, Lückerrath K, Kleinlein I, et al. ⁶⁸Ga-Pentixafor-PET/CT for Imaging of Chemokine Receptor 4 Expression in Glioblastoma. *Theranostics* 2016; 6(3): 428-434

25. Herhaus P, Lipkova J, Lammer F, et al. CXCR4-Targeted PET Imaging of Central Nervous System B-Cell Lymphoma. *J Nucl Med* 2020; 61: 1765-1771

FIGURE

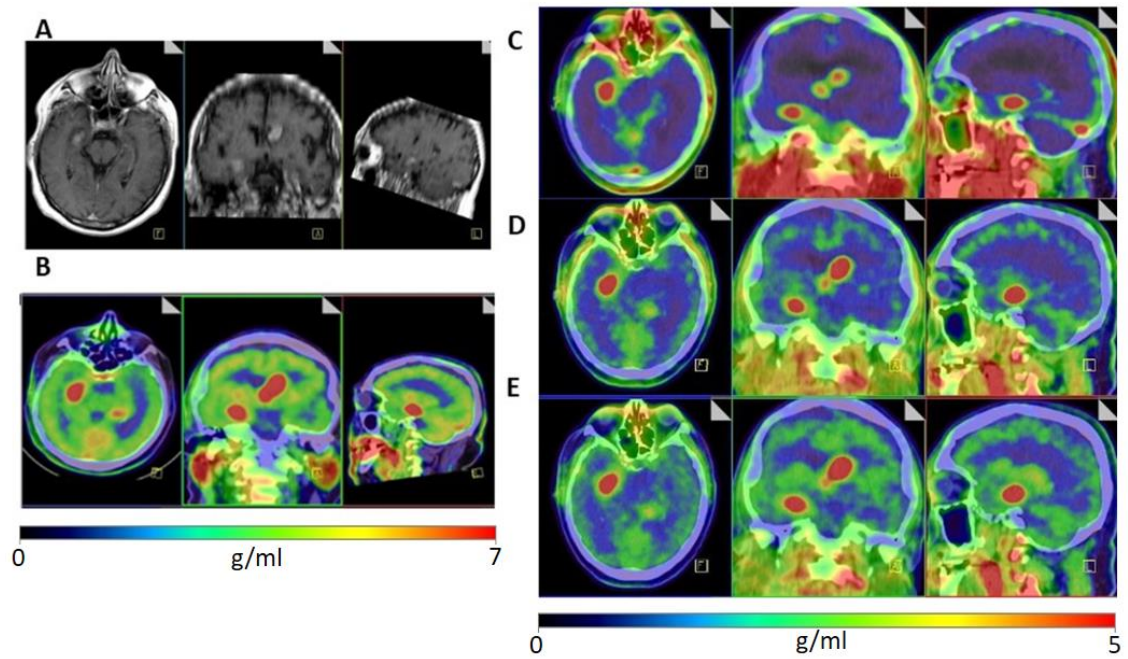


Figure 1: Representative patient harboring a primary CNS lymphoma (PCNSL). A) T1w+Gd MRI; B) Static C-11 MET (10-30 min); C-D-E): Static F-18 FLUDA images at 3-10 min, at 40-60 min, and at 100-120min.

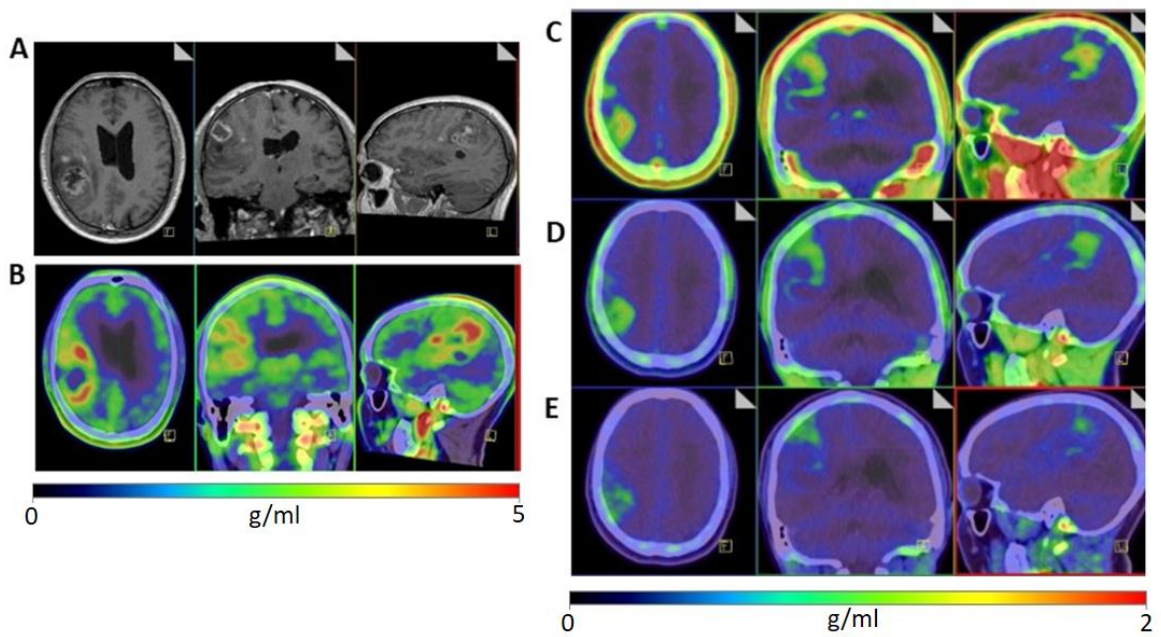


Figure 2: Representative patient harboring a glioblastoma. A) T1w+Gd MRI; B) Static C-11 MET (10-30 min); C-D-E): Static F-18 FLUDA images at 3-10 min at 40-60 min, and at 100-120min.

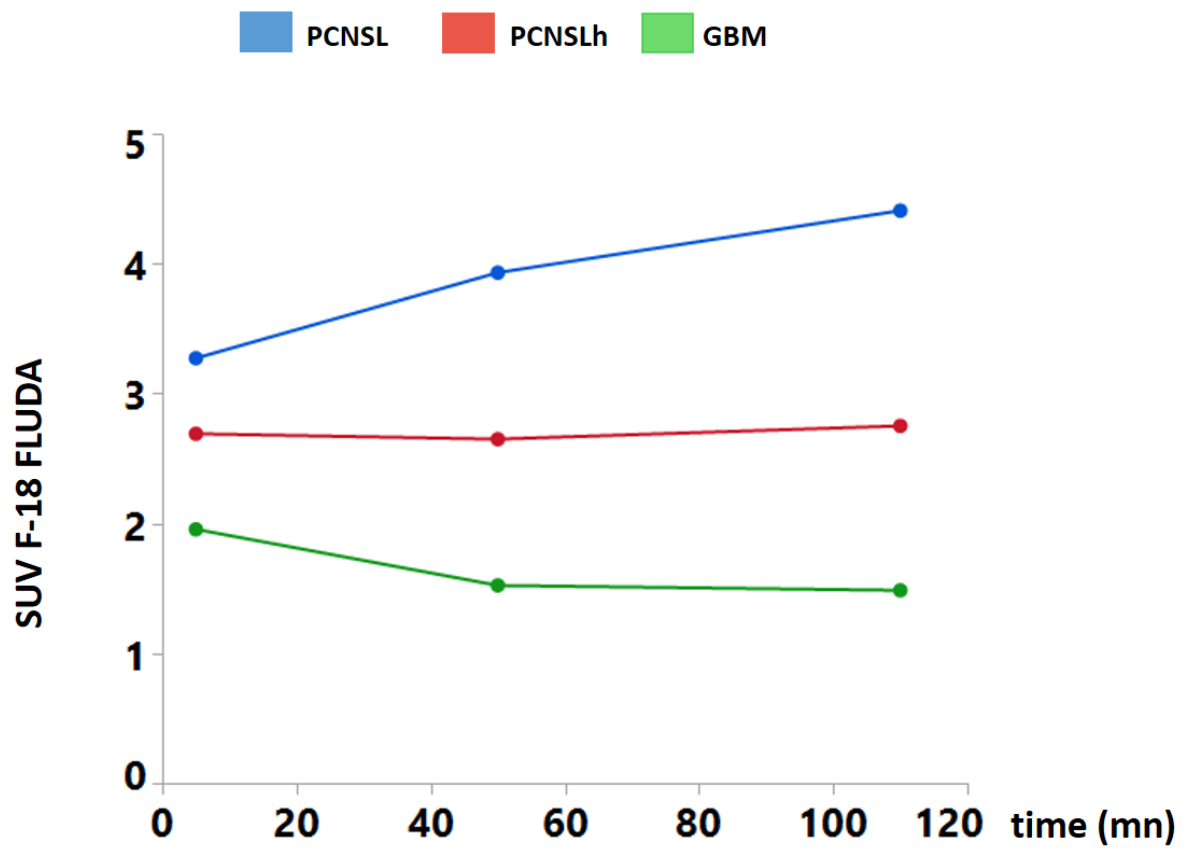


Figure 3: Dynamic data of F-18 FLUDA. Radiotracer uptake of F-18 FLUDA expressed as tumor to healthy tissue ratio (T/N) for PCNSL, PCNSLh, and GBM.

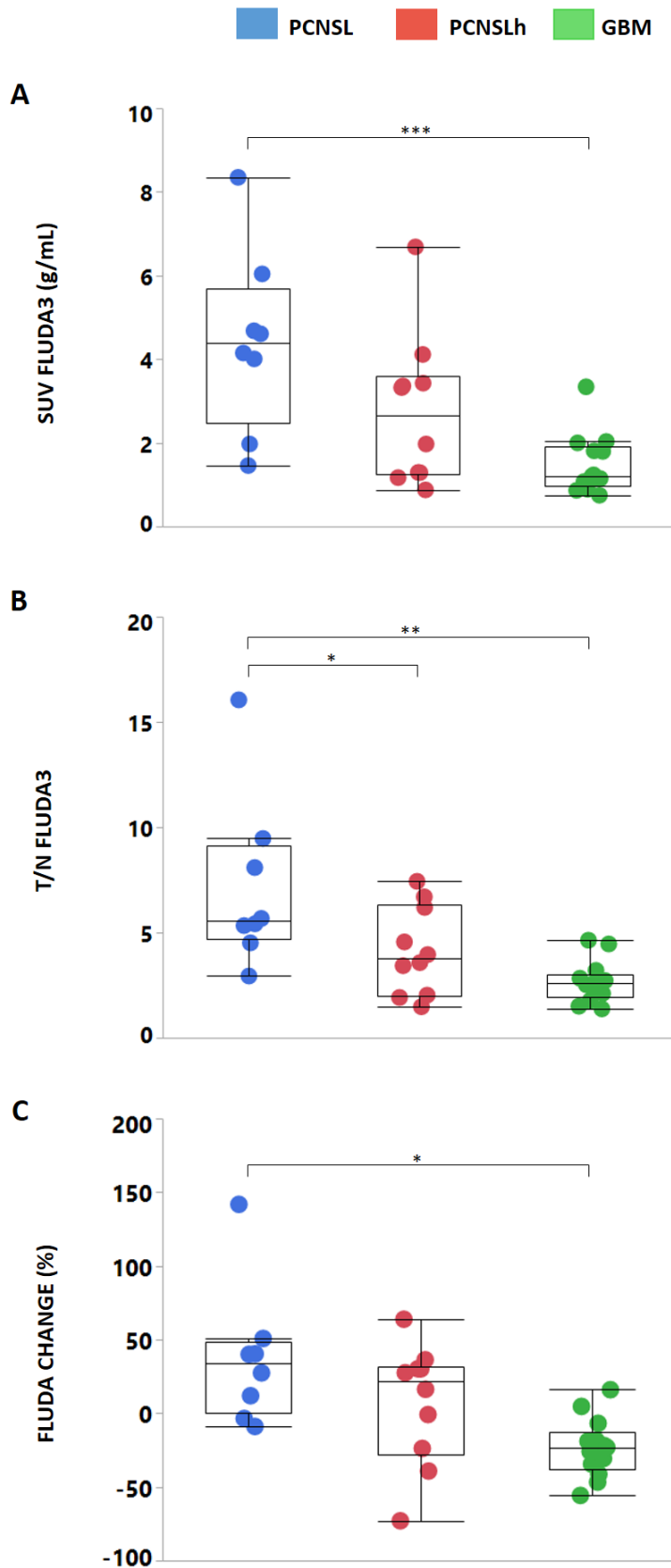


Figure 4: F-18 FLUDA uptake measurement without incorporating perfusion data. Radiotracer uptake of F-18 FLUDA at 100-120 min expressed as (A) SUV in tumors, (B) tumor to healthy tissue ratio (T/N), and (C) F-18 FLUDA Change between Time1 (0-10 min) and Time3 (100-120 min).

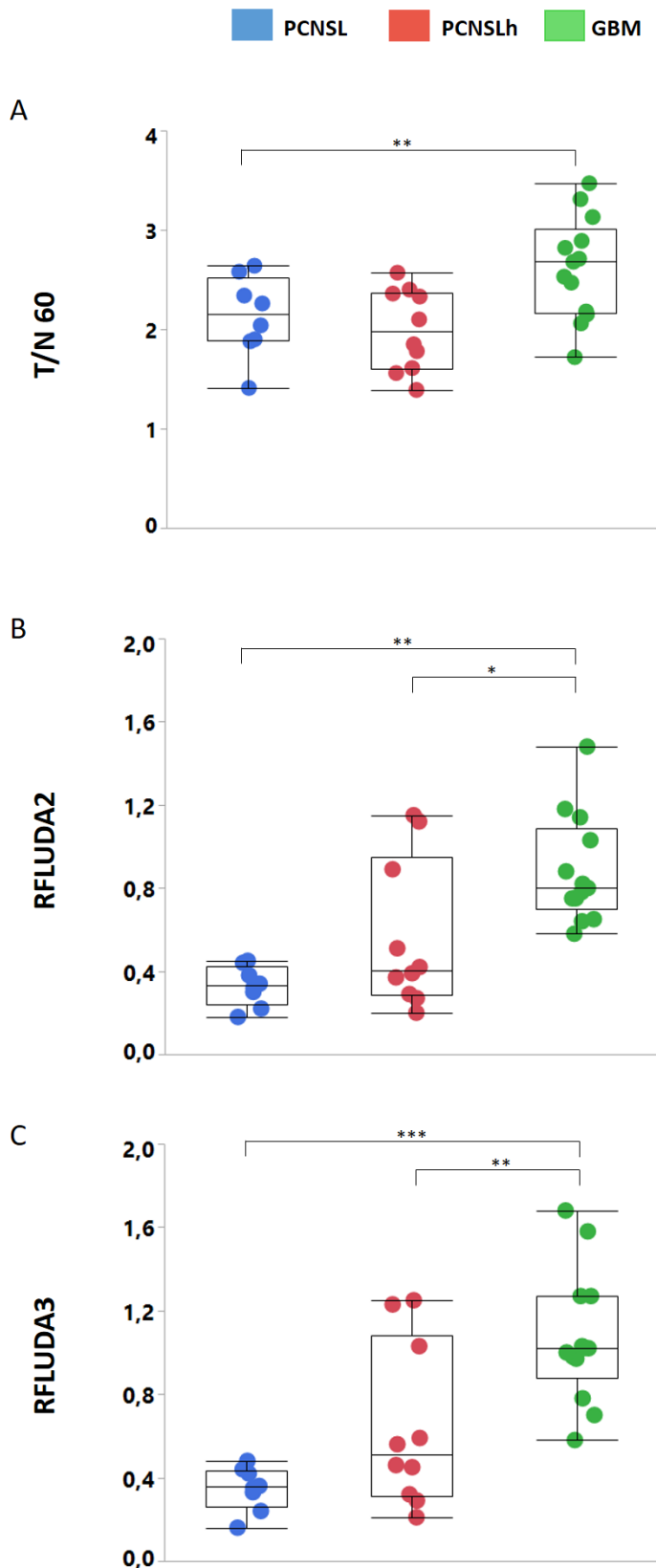


Figure 5: F-18 FLUDA uptake measurement weighted by perfusion data. Radiotracer uptake of F-18 FLUDA expressed as (A) tumor to healthy tissue ratio during the first min (T/N60), (B) the ratio of T/N FLUDA2 (40-60 min) to T/N60 as RFLUDA2 and (C) the ratio of T/N FLUDA3 (100-120 min) to T/N60 as RFLUDA3.

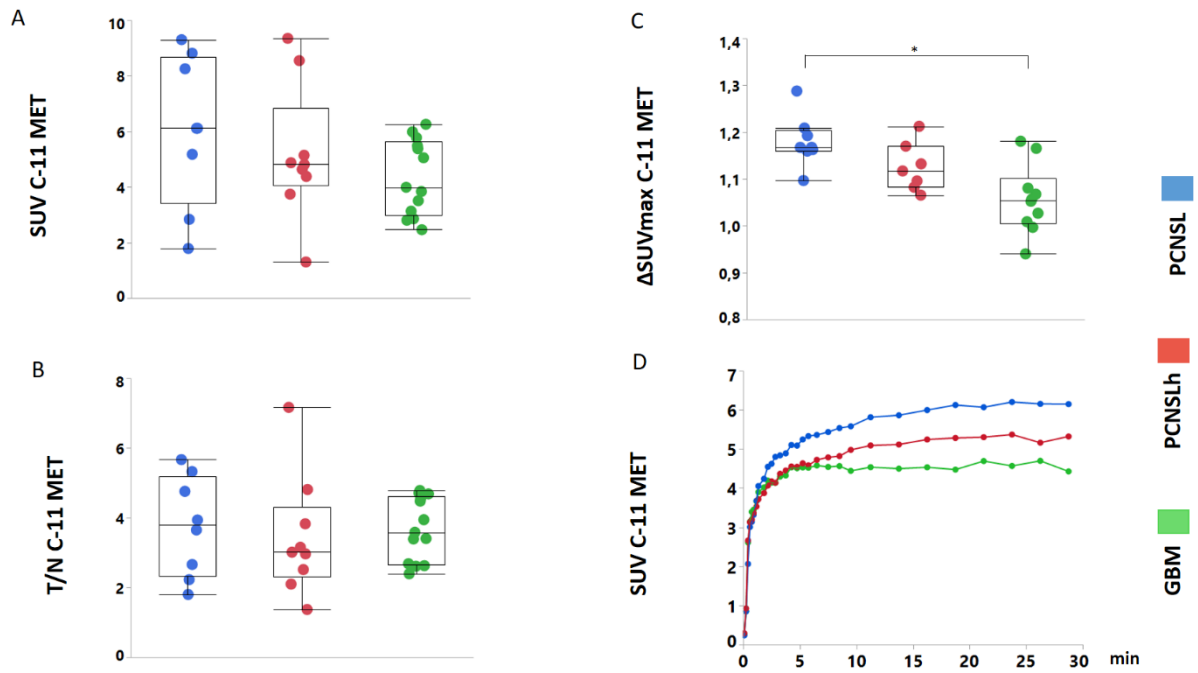


Figure 6: C-11 MET uptake measurement. Radiotracer uptake of C-11 MET at 0-30 min expressed as (A) SUV in tumors, (B) tumor to healthy tissue ratio (T/N), (C) comparison of early and later uptake, with $\Delta\text{SUV}_{\text{max}} = \text{averaged SUV}_{(20-30 \text{ min})} / \text{averaged SUV}_{(0-20 \text{ min})}$ and (D) radiotracer uptake of C-11 MET expressed as tumor to healthy tissue ratio (T/N) for PCNSL, PCNSLh, and GBM.

		PCNSL	PCNSLh	GBM
SUV 18F-FLUDA	FLUDA 1	3.27 (1.35)	2.69 (1.36)	1.95 (0.86)
	FLUDA 2	3.93 (1.79)	2.65 (1.66)	1.52 (0.64)
	FLUDA 3	4.41 (2.18)	1.75 (1.81)	1.49 (0.71)
T/N 18F-FLUDA	FLUDA 1	6.56 (2.04)	5.35 (2.30)	4.43 (1.67)
	FLUDA 2	7.37 (3.71)	4.67 (2.20)	3.17 (0.98)
	FLUDA 3	7.19 (4.12)	4.13 (2.08)	2.67 (1.00)
	FLUDA Change	37.47 (47.31)	6.74 (41.11)	-23.33 (19.91)
SUV 18F-FLUDA	T/N 60	2.13 (0.41)	2.00 (0.41)	2.62 (0.51)
	R FLUDA 2	0.33 (0.10)	0.56 (0.35)	0.88 (0.26)
	R FLUDA 3	0.35 (0.11)	0.64 (0.39)	1.07 (0.32)
11C-MET	SUV 11C-MET	6.05 (2.73)	5.20 (2.42)	4.35 (1.35)
	T/N 11C-MET	3.75 (1.44)	3.43 (1.71)	3.68 (0.91)
	ΔSUV _{max} 11C-MET	1.18 (0.05)	1.13 (0.05)	1.06 (0.07)

Table 1: Summary of the various metrics measured per group for 18F-FLUDA and 11C-MET (mean and standard deviation).

		ANOVA	PCNSL vs PCNSLh	PCNSL vs GBM	PCNSLh vs GBM
SUV 18F-FLUDA	FLUDA 1	>0.05	NS	NS	NS
	FLUDA 2	0.0020	NS	0.0014	NS
	FLUDA 3	0.0012	NS	0.0008	NS
T/N 18F-FLUDA	FLUDA 1	>0.05	NS	NS	NS
	FLUDA 2	0.0017	NS	0.0011	NS
	FLUDA 3	0.0014	0.0363	0.001	NS
	FLUDA Change	0.0028	NS	0.002	NS
SUV 18F-FLUDA	T/N 60	0.0065	NS	0.0076	NS
	R FLUDA 2	0.0003	NS	0.0002	0.0208
	R FLUDA3	<0.001	NS	<0.0001	0.0069
11C-MET	SUV 11C-MET	>0.05	NS	NS	NS
	T/N 11C-MET	>0.05	NS	NS	NS
	ΔSUV _{max} 11C-MET	0.0015	NS	0.0011	NS

Table 2: ANOVA and p values obtained after HSD Tukey Post-hoc test for the various metrics analyzed for 18F-FLUDA and 11C-MET.

	AUC	cutoff	sensitivity	specificity
SUV FLUDA3	0.923	2.43	75%	75%
T/N FLUDA3	0.961	4.51	87.5%	80%
FLUDA CHANGE	0.942	8.943	100%	76.9%
T/N 60	0.77	2.64	100%	53.8%
R FLUDA2	1	0.45	100%	100%
R FLUDA3	1	0.48	100%	100%
ΔSUV_{max} 11C-MET	0.9	1.10	100%	80%

Table 3: ROC analyses of the main metrics used in the study (GBM vs PCNSL).